Gold and platinum microclusters and their anions: Comparison of structural and electronic properties

ARTICLE *in* CHEMICAL PHYSICS · DECEMBER 2000

Impact Factor: 1.65 · DOI: 10.1016/S0301-0104(00)00294-9

ELSEVIER

Chemical Physics 262 (2000) 1–14

Chemical Physics

www.elsevier.nl/locate/chemphys

Gold and platinum microclusters and their anions: comparison of structural and electronic properties

Henrik Grönbeck, Wanda Andreoni *

IBM Research Division, Zurich Research Laboratory, CH-8803 Rüschlikon, Switzerland

Received 20 August 2000

Abstract

We present a study of Au_2 to Au_5 and Pt_2 to Pt_5 clusters within density-functional theory in the neutral and anionic states. Results obtained using two exchange-correlation (xc) functionals, local spin density approximation and spin-polarized Becke–Lee–Yang–Parr (BLYP), are compared. The structural characteristics and relative stabilities of different isomers as well as electron affinities and vertical detachment energies are calculated. The latter compare generally well with experimental data, especially in the BLYP case. However, strong dependence of the vertical electron detachment energies on the isomer and on the xc-functional scheme indicates that special care must be taken for any comparison of theoretical results with experiment. Both for platinum and gold tetramers and pentamers, 3D geometries are unfavored. Triplet states are predicted to be more stable than singlets for platinum, for all sizes considered. The relative stability of different geometrical isomers is strongly affected by the addition of one electron. Marked differences emerge in the electronic structure between the clusters of these two metals.

1. Introduction

Small metal clusters, and in particular their electronic and geometrical properties, have been thoroughly studied during the past decade using diverse spectroscopies and theoretical methods [1]. Whereas remarkable advances have been made in the theoretical approach, especially using calculations based on density-functional theory (DFT) [2,3], the current understanding of noble- and transition-metal clusters is unsatisfactory [4]. In the case of transition-metal clusters, there is no doubt that the complexity of their electronic structure, the description of which needs a correct inclusion of electron correlations and an accuracy capable of deciding between several quasi-degenerate low-lying electronic states as well as geometrical isomers, renders the investigation particularly challenging. Being the natural bridge between "simple" and transition-metal clusters, noble-metal aggregates constitute an interesting ground for the testing of theoretical and computational approaches, and should be less problematic. However, also in this case only a few attempts have so far been made. The study of heavy metals such as platinum and gold requires the inclusion of relativistic effects – another interesting problem. Moreover, platinum and gold are the most common constituents of nanostructured materials,

* Corresponding author. Tel.: +41-1-724-8344; fax: +41-1-724-8958.

E-mail address: and@zurich.ibm.com (W. Andreoni).

0301-0104/00/$ - see front matter
PII: S0301-0104(00)00294-9

with promising technological applications [5–9]. In most cases, the structural and specific electronic characterizations of these nanoscale systems are still difficult so that one must rely on the predictive power of computational methods. Therefore, it is important to establish the performance on the microclusters of relatively simple DFT-based methods that have been successful for the study of simple metal clusters and that also allow large sizes to be treated [10,11]. In this paper, we present a DFT study of microclusters of gold and platinum, both neutral and anionic, ranging from the dimer to the pentamer, using both the local spin density approximation (LSDA) for the exchange-correlation (xc) functional and the spin-polarized gradient-corrected Becke–Lee–Yang–Parr (BLYP) one. This comparative study of these two schemes for metal clusters can be considered an extension of the one we made for niobium clusters in Ref. [12] (see also Ref. [13]). [1] Structural properties and energetics of a number of isomers are considered. Electronic properties are discussed, and the effects of the addition of one electron on the structure are investigated in the anions. Adiabatic electron affinities (EA_a) as well as vertical electron detachment energies (VDEs) are computed, and the latter compared with photoemission data (Pt [14–16] and Au [17–19]).

2. Computational method: justification and criticism

All calculations were performed with two different functionals for the exchange and correlation energy, both including spin polarization: LSDA with the Perdew–Zunger parametrization [20] of the Ceperley–Alder results for the electron gas [21], and the so-called BLYP approximation, which includes density gradient corrections to the local Slater exchange as proposed by Becke [22], and the Lee–Yang–Parr expression [23] for the correlation energy functional. The DFT implementation we use treats the core–valence interaction with pseudopotentials, and expands the wave functions of the valence electrons in plane waves [24]. [2] Norm-conserving, angular-momentum-dependent pseudopotentials were generated with the method of Troullier and Martins [25], and derived from scalar relativistic all-electron calculations. In this way, they account for those relativistic effects that in our case are most dramatic, namely, the contraction of the s-wave functions and the expansion of the d-wave functions. For platinum we used an 18-electron pseudopotential that was previously applied to the study of Pt(II) complexes [26]. [3] Core radii for the s, p and d components were 1.1, 1.2 and 1.24 a.u., respectively; the s component was used as the local part. For gold an 11-electron pseudopotential was tested, with s, p, and d radii of 2.35, 2.35, and 1.5 a.u., respectively; the s component was taken as the local part. An application of this pseudopotential to the study of chemisorption on the gold (1 1 1) surface and on a 38-atom cluster is reported in Refs. [11,28].

Inclusion of core shells in the "active" orbital space (semi-core pseudopotential) is mandatory for both Pt and Au. For example, in the case of gold clusters, a one-electron pseudopotential that we constructed with the Trouiller–Martins procedure including non-linear core corrections [29] underestimated bond lengths by ~25% and overestimated bond strengths by ~35%. To identify the specific consequences the inclusion of scalar relativistic terms in the core–valence interaction has on the cluster properties, we have also constructed pseudopotentials with the same procedure as above, but starting from non-relativistic all-electron calculations. The main effects were contraction of the bond lengths, enhancement of the cohesive energies, and a global hardening of the vibrational spectra. This agrees with the conclusions previously drawn from calculations of Au_2 using other methods [30,31]. As mentioned, our computational approach includes relativistic effects only partially and in particular does not

[1] A comparison of LDA and Perdew–Wang GGA is made for Cu_n microclusters in Ref. [13].

[2] We used the CPMD code in the parallel IBM version 2.5 developed by J. Hutter (copyright IBM).

[3] A similarly constructed pseudopotential, in the Becke–Perdew xc-functional scheme, was applied to Pt carbonyls [27].

include spin–orbit (SO) coupling. The assessment of the influence of the SO coupling is generally still incomplete, and limited to the dimers. For instance, a study of the platinum dimer [32], using complete active space (CASSCF) calculations followed by first-order configuration interaction (FOCI), indicates that SO interaction effects could be as large as 0.7 eV for dissociation energies. For the gold dimer, on the other hand, variations seem to be much less dramatic, see e.g. Refs. [33,34]. We shall mention some of these findings in the following section. The importance of SO coupling will, however, depend on the specific cluster property. For example, a number of calculations were performed to establish such effects on the hyperfine interaction of small metal clusters [35] using the zeroth-order regular approximation [36] to the Dirac–Kohn–Sham equation to include SO coupling in the DFT formalism (with gradient-corrected Becke–Perdew [22,37] functionals). In the case of the gold heptamer, the SO coupling effects appear to be crucial because they modify the character of the singly occupied molecular orbital in an important way.

Our calculations were performed using a 25-a.u.-edge cubic cell free of periodic boundary conditions [38], a plane wave cutoff of 70 Ry in the case of platinum and of 50 Ry in the case of gold. Some tests have been made with a larger cell and higher energy cutoff. We have also verified that softer pseudopotentials, especially for the "d" components indeed alter the output and result in inaccurate predictions. The wave functions were optimized with the direct inversion in iterative subspace (DIIS) method [39,40]. DIIS in combination with a quasi-Newton method was used to optimize the atomic positions. All reported structures are converged to within 5×10^{-4} a.u., at least for the largest element of the gradient.

Only electron states of low spin multiplicity (singlets (S) and triplets (T)) have been considered for systems with an even number of electrons. For the gold microclusters this is probably a minor limitation as the d shell is filled and the s electrons are delocalized. For the platinum clusters, however, it may very well be a limitation. In fact, previous work on the Pt dimer [32], trimer [41], and tetramer [42] revealed that higher spin states may be relevant, because several electronic states of different multiplicity were close in energy.

3. Results

The results of our calculations are reported below, and compared with previous first-principles calculations. Comparison with experiment is necessarily limited to the ground-state characteristics of the dimer, some electron spin resonance (ESR) data and mainly PES measurements of the VDEs. The VDE is computed as the total energy difference between the anionic and the neutral cluster, with the neutral cluster in the geometrical configuration of the anion. The EA_a, in contrast, is the energy difference between the charged and the neutral clusters in their ground-state structures. Whereas the former measures the effect of the electron relaxation, the latter includes also that of structural relaxation. Such structural changes are illustrated directly in the figures.

3.1. Gold clusters: Au_2 to Au_5

Our results for the spectroscopic constants of the gold dimer are shown in Table 1. The LSDA output is in excellent agreement with that of previous LDA calculations in Ref. [31], where a scalar relativistic approach based on a unitary Douglas–Kroll transformation and an expression of the electronic wave functions in terms of linear combinations of Gaussian type of orbitals (LCGTO) were used. This is true only in part for the comparison with the pseudopotential–cylindrical wave computations of Ref. [43], owing to the large difference (0.38 eV) in the value reported for the binding energy. This can be attributed to the neglect of spin polarization of the separated atoms in Ref. [43], which we find to be 0.15 eV per gold atom and which thus would account for a 0.30 eV difference. The LSDA values for the bond distance and the stretch vibration frequency compare well with experimental data [44]. However, the binding energy is overestimated, as expected. A substantial improvement is found with the BLYP functional scheme: the bond distance expands by a few

Table 1
Characteristics of Au_2 and Pt_2 in their ground states

Method	Au_2 (singlet)			Pt_2 (triplet)		
	d (a.u.)	D (eV)	ω (cm^{-1})	d (a.u.)	D (eV)	ω (cm^{-1})
LSDA (this work)	4.68	2.87	195	4.26	4.92	267
BLYP (this work)	4.84	2.10	173	4.38	3.58	239
LDA[a]	4.67	2.88	195	–	–	–
LDA[b]	4.63	3.25	193	–	–	–
FOCI[c]	–	–		4.64	1.95	189
CCSD(T)-DKH[d]	4.70	2.19	187			
Exp.	4.67[e]	2.30[e]	191[e]	–	3.71[f], 3.14[g]	215[h]

[a] Ref. [31].
[b] Ref. [43].
[c] Ref. [32].
[d] Ref. [34].
[e] Ref. [44].
[f] Ref. [52].
[g] Ref. [53].
[h] Ref. [61].

percent and the vibrational frequency reduces by $\sim$10%.

As mentioned in Section 2, relativistic effects have been included in a number of studies of the gold dimer, beyond the scalar approximation. These were recently reviewed in Ref. [34], which also reported progress made by using high-level first-principles calculations: the coupled-cluster approach and the Douglas–Kroll–Hess (DKH) transformation of the Dirac operator. Variations with respect to other non-relativistic coupled-cluster calculations seem to be minor. Within DFT, fully relativistic calculations are reported in Ref. [33], that are made within an all-electron frozen-core scheme using Becke [22] and Perdew [37] gradient-corrected functionals. Unfortunately, on the basis of our findings, we see that the accuracy of these calculations, when compared to experiment, suffers from having the d shell frozen. Thus their result cannot be conclusive. However, from all the above, it is clear that, given the uncertainty of all other approximations included in typical DFT calculations, the effects of neglecting SO coupling are minor on the properties we are interested in here.

The structures of the low-energy isomers for the gold trimer, tetramer, and pentamer are shown in Fig. 1. The energy separations between the isomers are compiled in Table 2. As expected for a three-electron system (for Na_3 [45], for Cu_3 [46] and for Ag_3 [47]) [48] the equilateral triangle (D_{3h} symmetry) is unstable with respect to a Jahn–Teller (JT) distortion. Depending on which of the degenerate states of the highly symmetric structure is populated, the distortion is either to an obtuse or an acute triangle. The energy difference between these two isomers is very small, so that the obtuse triangle is only slightly more stable. The energy gain associated with the JT distortion amounts to 0.01 eV in LDA and 0.03 eV in BLYP. [4] The linear configuration (3c) is clearly separated from the two triangular isomers in both LDA and BLYP. Although direct information on the gas-phase trimer is not available, the obtuse triangle has indeed been suggested by early ESR measurements [49] on Au_3 embedded in a benzene matrix. A great discrepancy is found, on the other hand, to CASSCF studies in Ref. [50], which predict the linear configuration as ground state and do not find the obtuse triangle to be a minimum of the potential energy surface. Again, one could partly ascribe this discrepancy to the neglect of d-electron correlation in Ref. [50].

[4] Highly symmetric structures such as the equilateral triangle or the regular tetrahedron could be numerically stabilized by imposing a uniform occupation of the degenerate states.

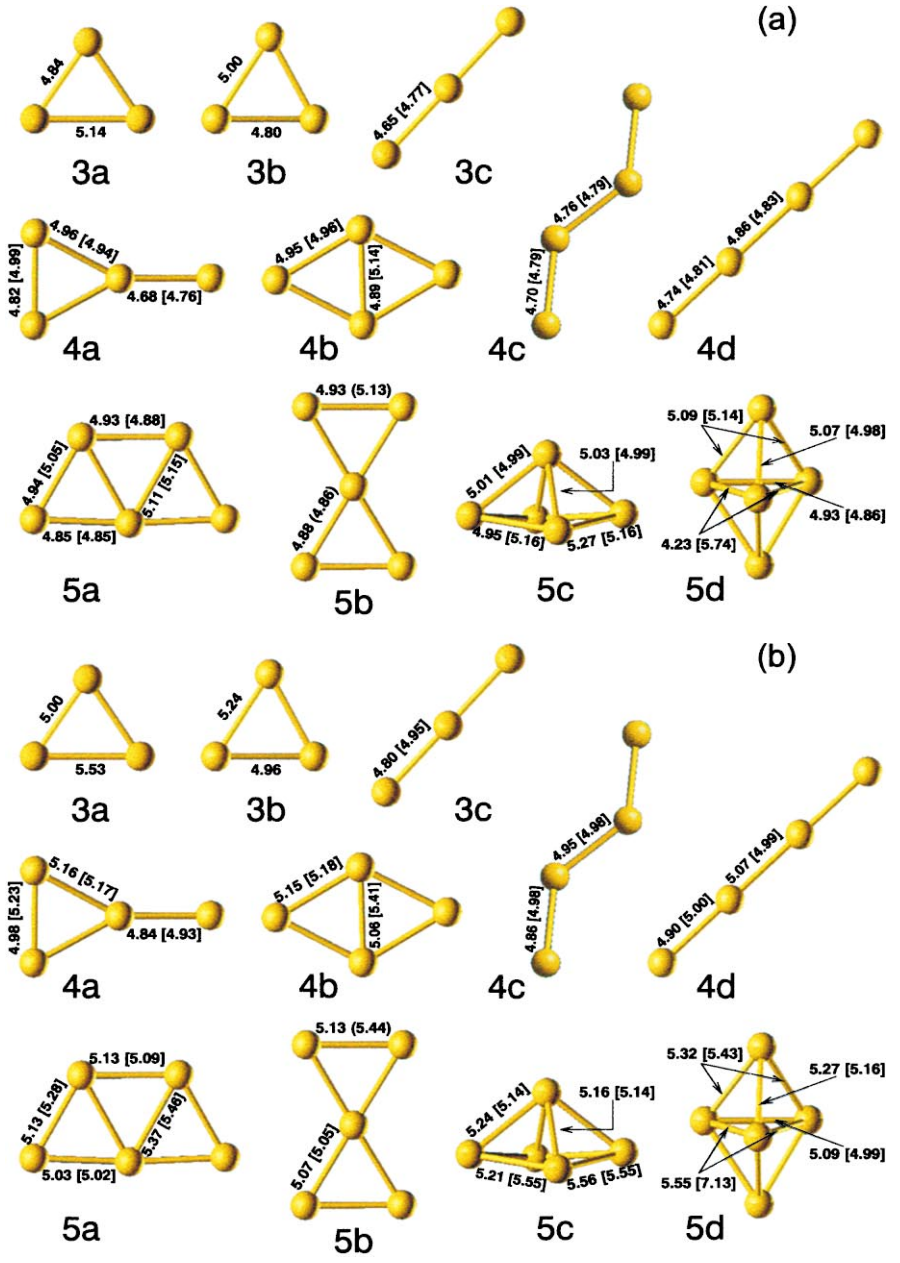

Fig. 1. Results for the low-energy structures of Au_3 to Au_5, obtained in (a) the LDA and (b) the BLYP schemes. The interatomic distances are reported in a.u.; the results for the anionic clusters are given within parentheses.

Four geometries are shown in Fig. 1 for the gold tetramer: a Y-shaped structure (4a), a rhombus (4b), a zig-zag (4c) and a linear (4d) chain. Whereas LDA clearly separates 4a and 4b, BLYP suggests the existence of an accidentally degenerate ground state for the neutral gold tetramer. Both the zig-zag and the linear structures are considerably higher in energy. Because of JT distortions, highly symmetric structures such as the square (D_{4h}) and the tetrahedron (T_d) are unstable

Table 2
Total energy separation of neutral ($\Delta E(0)$) and anionic ($\Delta E(-)$) gold clusters Au_2 to Au_5 together with corresponding VDE and EA_a[a]

	LSDA				BLYP				Exp.[b]
	$\Delta E(0)$	$\Delta E(-)$	EA_a	VDE	$\Delta E(0)$	$\Delta E(-)$	EA_a	VDE	VDE
Au_2	–	–	2.21	2.26	–	–	2.01	2.08	2.02
Au_3(a)	0	–	–	–	0	–	–	–	3.85
Au_3(b)	0.01	–	–	–	0.02	–	–	–	
Au_3(c)	0.41	0	4.21	4.26	0.12	0	3.82	3.87	
Au_4(a)	0.27	0.12	2.94	2.99	0	0.20	2.73	2.78	2.77
Au_4(b)	0	0	2.79	2.84	0.01	0.40	2.54	2.61	
Au_4(c)	0.87	0.21	3.45	3.69	0.28	0	3.21	3.39	
Au_4(d)	1.41	0.38	3.82	3.84	0.67	0.13	3.48	3.49	
Au_5(a)	0	0	3.33	3.35	0	0	3.04	3.08	3.12
Au_5(b)	0.63	0.89	3.07	3.13	0.34	0.55	2.82	2.92	
Au_5(c)	0.87	0.88	3.32	3.39	1.00	1.05	2.99	3.14	
Au_5(d)	0.72	1.14	2.91	3.05	1.03	1.25	2.83	2.94	

[a] All energies are in eV. Only singlet states are reported for Au_2 and Au_4. Au_3 and Au_5 are doublets.
[b] Ref. [17].

in the singlet state. For the square, the triplet state is found to be a local minimum, but significantly higher than the ground state (0.82 eV in LDA, 0.60 eV in BLYP). The regular tetrahedron[4] is much higher than 4a both at the LDA (1.47 eV) and BLYP (1.83 eV) levels. Multireference calculations including single and double excitations (MRSDCI) [50] predict a rhombus (4b) as the lowest-energy isomer (with a 5.08-a.u. edge; see Fig. 1 for comparison). At first sight, this could be considered in agreement with our LDA results. However, the 4a isomer was not considered at all in Ref. [50]. Also, the D_{4h} triplet was found to be 1.17 eV higher than 4b, whereas in LDA it is higher by 0.82 eV.

The Au_5 cluster is also found to prefer planar structures. Both LDA and BLYP suggest 5a as the ground state, i.e. the most compact possible planar configuration, in analogy to the pentamers of alkali metals and silver [4]. The more open X-shaped geometry (5b) is less unfavored in BLYP than in LDA. We have considered two highly symmetric 3D structures, namely, the square pyramid (C_{4v}) and the regular trigonal bipyramid (D_{3h}). They turn out to be unstable and result both in C_{2v} geometries (5c and 5d, respectively). The distortion in 5d with respect to the trigonal bipyramid consists of the shortening of one of the bonds in the equatorial triangle and is consistent with the nature of the highest occupied molecular orbital (HOMO), a bonding orbital between the two atoms forming the short bond. The D_{3h} isomer is unstable, and decays into a C_{2v} structure, which is the same for BLYP and LDA.

Fig. 2 shows the electronic density of states (DOS) of the lowest-energy isomers for Au_2 to Au_5, and its global projection (PDOS) on the 6s and 6p atomic pseudo-wave functions. This plot refers to the BLYP results. The two even-numbered clusters, Au_2 and Au_4, have large HOMO–LUMO (LUMO: lowest unoccupied molecular orbital) separations of 1.8 and 0.9 eV, respectively. This is consistent with PES measurements [17] of the anions, which indicate a larger separation between the first and second main peak in the spectra for the even-sized clusters. For the odd-numbered clusters, the HOMO–LUMO separations are much smaller, namely, 0.2 and 0.3 eV for Au_3 and Au_5, respectively.

The PDOS reveals that the unoccupied states in a range of 4 eV above the HOMO are of sp character for all cluster sizes. More precisely, only for states higher than $\sim$2 eV above the HOMO level does the 6p contribution become sizable. With the exception of Au_2, the HOMO level is predominantly of s character. For Au_2, the HOMO is an antisymmetric combination of the

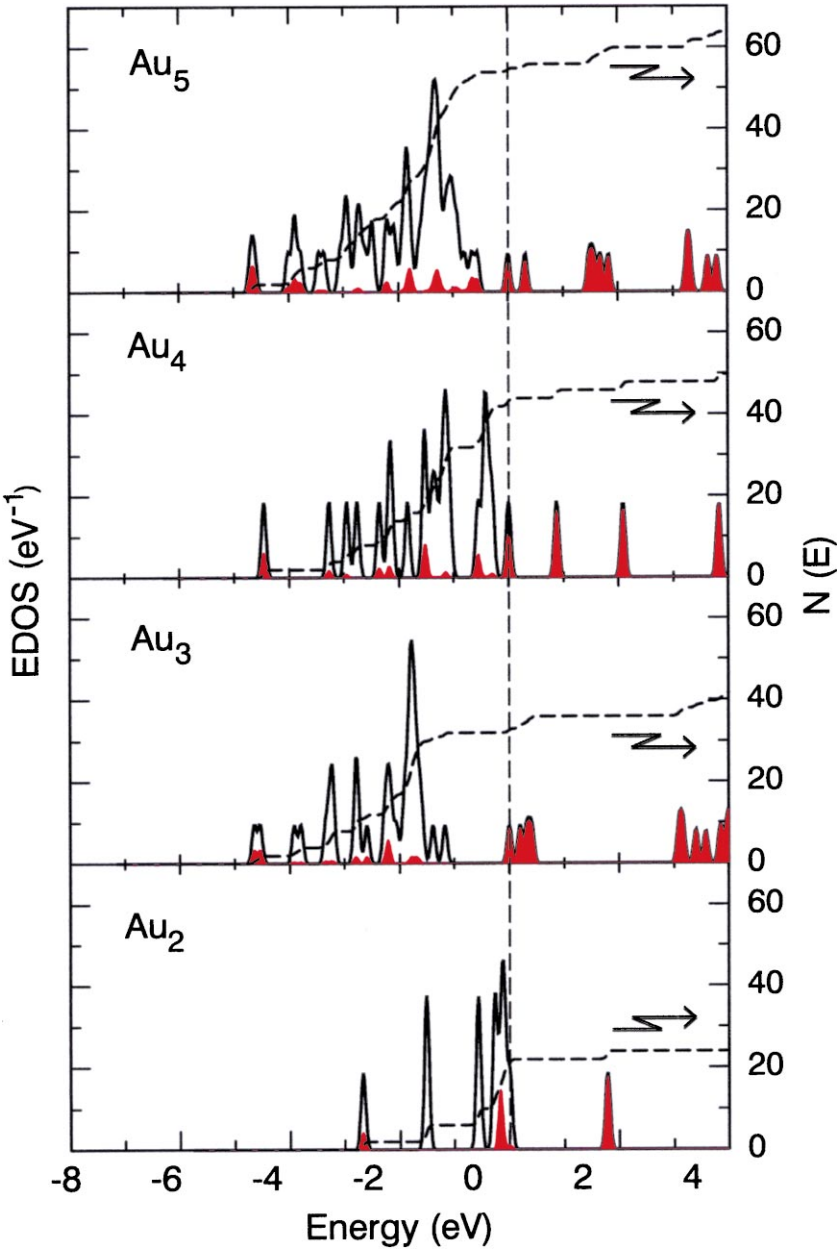

Fig. 2. Au_n clusters: density of valence electron states for the lowest-energy isomers. Energies refer to the HOMO level. Dashed line shows integrated total DOS. The filled spectrum corresponds to the projection on the sp orbitals. The one-electron Kohn–Sham levels are broadened with a 0.1-eV Gaussian.

atomic d_{z^2} orbitals. Even for this very limited cluster range an interesting trend regarding the character of the lowest-lying valence state is present. For the dimer, the 6s character is only 20%, whereas it is close to 50% for the pentamer. For much a larger cluster size, such as Au_{38}, the 6s contribution dominates [11]. A Mulliken population analysis reveals that for all cluster sizes, the

"effective population" is close to $d^{9.9}s^{1.0}p^{0.1}$. The existence of a fully occupied d shell does not imply that the d contribution to the bonding is small. As revealed by PDOS, the hybridization between d and s states is substantial.

Our results for the energy separation of the negatively charged cluster isomers are also collected in Table 2. With respect to the neutral clusters, there are important changes in the ordering of the isomeric structures: For the trimer the triangles become unstable upon charging. For the tetramer dramatic changes in the energy ordering take place in the BLYP scheme, and the zig-zag structure turns out to be the ground state. For the pentamer, the planar C_{2v} isomer becomes more stable in comparison with the other isomers investigated, and the 3D structures lose stability. The addition of one electron to 5c stabilizes the square pyramid against the distortion in the neutral cluster (still reported as (5c) in Fig. 1). Regarding the distorted trigonal bipyramid (5d), the two equatorial bonds are loosened by the extra electron. However the enlargement is 10% in LDA, whereas in BLYP it is as much as 28%.

In Table 2 we report the VDE and the EA_a. The effect of structural relaxation is less than 0.1 eV in all cases except for the 3D structures of Au_5. Included in Table 2 are the experimental results for the VDEs of Ref. [17]. Excellent agreement is obtained at the BLYP level for the lowest-energy isomer for the dimer, trimer and pentamer. For the tetramer, however, the computed VDE for the chain structures are so much higher than the measured VDE that, on the basis of the BLYP result, it seems reasonable to conclude that the isomer distribution in the cluster beam is dominated by one or both of the other two isomers. In the LDA scheme, the conclusion would be completely different, because the VDE corresponding to the lowest-energy isomer is in very good agreement with the experimental one. The application of another xc-functional scheme at this point could be valuable. However, it would be also worthwhile to perform molecular dynamics simulations so as to explicitly take into consideration the effect of temperature on the population of the different isomers.

3.2. Platinum clusters: Pt_2 to Pt_5

The characteristics of the neutral dimer are listed in Table 1. The ground state of Pt_2 is a triplet. The singlet state turns out to be $\sim$0.7 eV higher in energy both in the LDA and in the BLYP schemes, with a bond distance only 0.03 a.u. larger than that of the triplet. To our knowledge, the bond length of Pt_2 has not yet been determined in the gas phase. Scanning tunneling microscopy measurements [51] of Pt_2 deposited on graphite give a value of 4.62 ± 0.5 a.u. Gas-phase data reported so far for the binding energy are significantly different: 3.71 eV on the basis of high-temperature equilibrium studies [52] and 3.14 eV measured with two-photon ionization experiments [53]. The LSDA result is clearly higher than both experimental data. Note that the ground state of the atom $Pt(d^9s^1)$ is also a triplet. CASSCF–FOCI calculations [32] (see Table 1) predict a dimer that is much more weakly bound, has a longer bond distance and a lower vibrational frequency. This result could be regarded as – at least in part – a sign of an incomplete treatment of the correlation.

The results of the structural optimization of the platinum clusters investigated are shown in Fig. 3, and the corresponding energy separations between the isomers are reported in Table 3.

For the trimer, the triangle is equilateral (D_{3h}) in the singlet state, and slightly distorted to an acute triangle in the triplet (Fig. 3). The energy separation between these two states is indeed small. The singlet is only 0.05 eV higher than the triplet in BLYP, and 0.07 eV lower in LDA. The linear isomer (3c) is clearly higher in energy, and has a triplet ground state in both LDA and BLYP. In the singlet state, the Pt–Pt bond lengths shrink by less than 1%.

Pt_3 has previously been investigated by generalized valence-bond calculations [41], with a relativistic 10e effective core potential [54], and a Gaussian basis for the expansion of the electronic wave functions. Ten low-lying electronic states were calculated to be within 0.28 eV. The lowest-energy isomer was proposed to be an acute triangle in the triplet state, 0.13 eV lower than the equilateral in the singlet state. This corresponds well to our findings in BLYP. However, the calculated

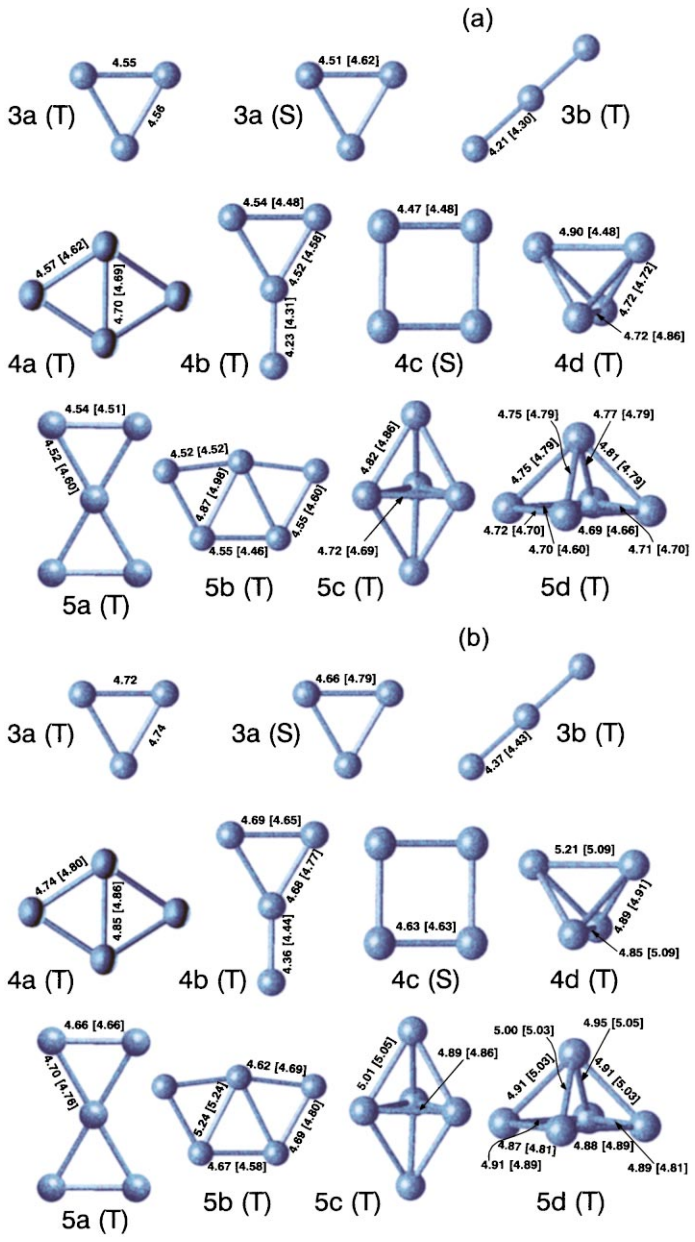

Fig. 3. Results for the low-energy structures of Pt_3 to Pt_5 obtained in (a) the LDA and (b) the BLYP schemes. The spin state is indicated by S for singlet and T for triplet. The interatomic distances are reported in a.u.; the results for the anionic clusters are given within parentheses.

bond-length values of 5.14 and 5.61 a.u. are 15% longer than ours. The lengthening of bond lengths is the expected outcome of calculations that only partially include electron correlation. In particular, we could verify that this large discrepancy is not due to the fact that in our pseudopotential scheme the 5s and 5p states are also treated as valence states. In fact, using a 10e pseudopotential, we find that the bond-length values increase by only $\sim$2%.

Table 3
Total energy separation of the neutral ($\Delta E(0)$) and anionic ($\Delta E(-)$) Pt_2 to Pt_5 together with corresponding VDE and EA_a[a]

		LSDA				BLYP				Exp.[b]
		$\Delta E(0)$	$\Delta E(-)$	EA_a	VDE	$\Delta E(0)$	$\Delta E(-)$	EA_a	VDE	VDE
Pt_2	T	–	–	2.00	2.05	–	–	1.70	1.74	1.9
Pt_3(a)	T	0.07	0.71	2.23	2.25	0	0.87	1.97	1.99	1.9
	S	0	–	2.16	2.23	0.05	–	2.02	2.09	
Pt_3(b)	T	0.26	0	3.13	3.18	0.19	0	3.03	3.05	
	S	0.40	–	3.27	3.35	0.23	–	3.07	3.14	
Pt_4(a)	T	0	0.44	2.56	2.61	0	0.77	2.19	2.29	2.6
	S	0.16	–	2.72	2.82	0.38	–	2.57	2.66	
Pt_4(b)	T	0.14	0	3.14	3.18	0.01	0	2.92	2.93	
	S	0.15	–	3.15	3.21	0.06	–	2.98	3.03	
Pt_4(c)	S	0.26	0.12	3.13	3.13	0.19	0.37	2.74	2.74	
Pt_4(d)	T	0.25	1.07	2.17	2.21	0.34	1.30	1.97	2.01	
Pt_5(a)	T	0.13	0.34	2.86	2.89	0	0.03	2.59	2.62	2.8
	S	0.40	–	3.15	3.19	0.34	–	2.93	2.98	
Pt_5(b)	T	0	0	3.07	3.11	0.35	0	2.97	3.03	
	S	0.15	–	3.23	3.27	0.44	–	3.06	3.11	
Pt_5(c)	T	0.31	0.53	2.84	2.92	0.53	0.72	2.43	2.48	
Pt_5(d)	T	0.11	0.49	2.69	2.72	0.54	0.74	2.42	2.45	

[a] All energies are in eV. The spin multiplicity (singlet (S) or triplet (T)) is indicated for the neutral clusters. Anions are all doublets.
[b] Refs. [15,16].

For the tetramer, (4a,C_{2v}) and (4b,C_{2v}) are the low-energy structures (quasi-degenerate in BLYP) of the neutral cluster. The 4a isomer is slightly out of the plane in the triplet and becomes a planar rhombus (D_{2h}) in the singlet. The Y-shaped isomer (4b) is planar. For this configuration, the singlet and triplet are quasi-degenerate. Of the high-symmetry structures, we find that the square is metastable in the singlet spin configuration (4c,D_{4h}). The regular tetrahedron is unstable, but a slight distorted one (4d,C_{2v}) is metastable in the triplet.

In Ref. [42], MRSDCI calculations were performed using 10 electrons in the valence space and relativistic effective core potentials that include SO interaction. The sequence and the type of relevant isomers found are different from the one predicted here. In fact, a regular tetrahedron in a triplet state was determined to be the ground state and split from the singlet state by 0.08 eV. The rhombus (threefold-degenerate ground state including singlet, triplet, and quintet states) and the singlet square are 0.47 and 0.64 eV higher, respectively. The 4b isomer was not considered at all.

For Pt_5, we find that all topologies investigated were triplets in the ground state. The two functionals give significantly differing answers as to the energy separation between the isomers. Whereas BLYP clearly predicts the lowest-energy isomer to be planar, LDA places the distorted "square" pyramid at low energies.

The present study is the first in which a range of cluster sizes for platinum has been investigated from first principles within one theoretical framework. Previously, the structural evolution of small platinum cluster has only been studied using the non-self-consistent Harris functional within LDA [55]. This approach is based on the assumption that binding energies can be evaluated using the electronic densities of the isolated fragments, in this case the atoms [56]. This is probably a crude approximation when treating systems for which the bond formation strongly perturbs the electron density distribution with respect to a simple superposition.

The electronic density of states of the lowest-energy isomers in the BLYP scheme is shown in Fig. 4. There is no noteworthy difference with the

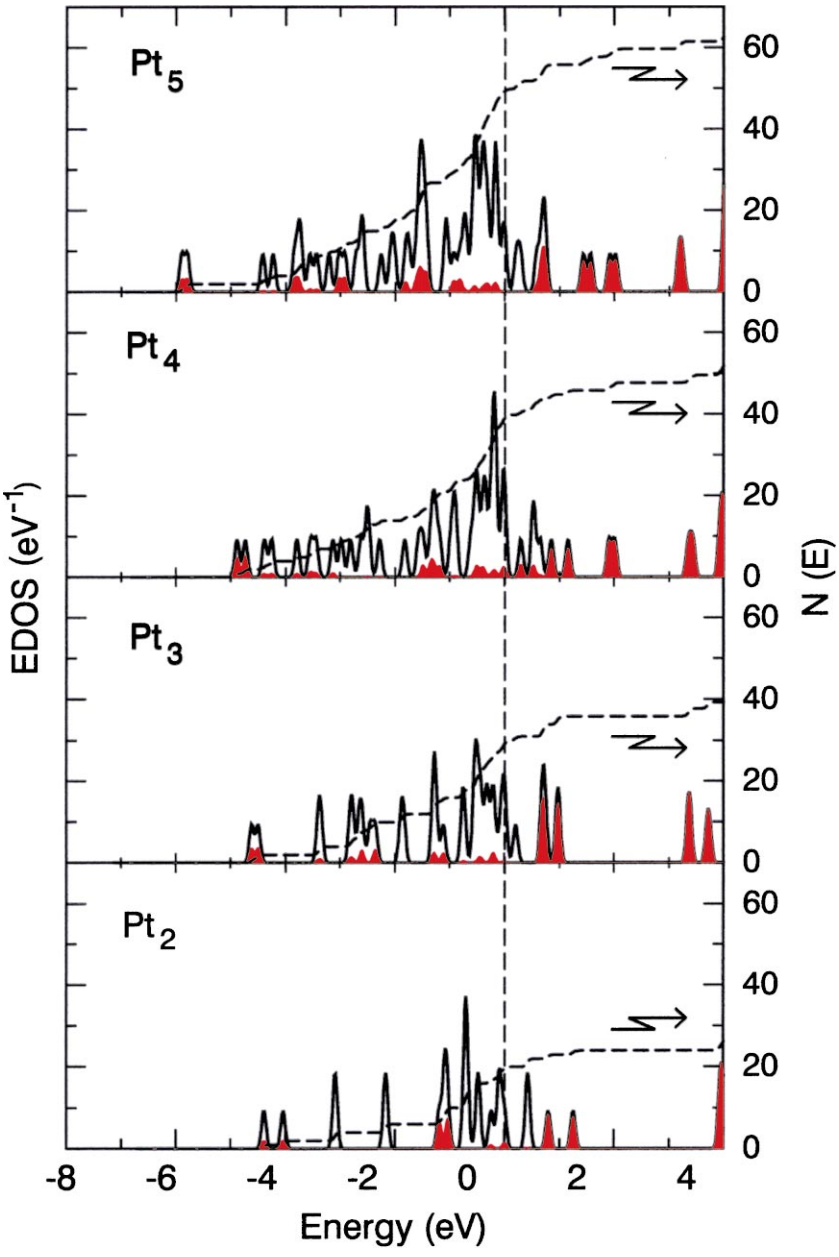

Fig. 4. Pt_n clusters: density of valence electron states of the lowest-energy isomers. The same description as for Fig. 2 applies.

LDA. The 5s and 5p states are much lower in energy and do not directly participate in the bonding. The energy spread of the low-lying states is strongly dependent on the isomer, with largest spread for the low-symmetry structures, as expected. On average the width is ~1 eV for the 5s states, and ~2 eV for the 5p states. The HOMO–LUMO separation is small in Pt_3, Pt_4 and Pt_5 (0.2, 0.3, and 0.2 eV), and larger in the dimer (0.7 eV). From the projected DOS we find that both

HOMO and LUMO levels are mainly of d character. The Mulliken population analysis for the lowest-energy isomers shows that the "average" electronic configuration is close to $d^{8.8}s^{1.1}p^{0.1}$ for the dimer, tetramer and pentamer. For the Pt_3 ground state the s contribution is weaker: $d^{9.1}s^{0.8}p^{0.1}$.

The results for the anionic clusters (Table 3) show again that important effects are driven by the addition of an electron on the isomer distribution. For the trimer, unlike the neutral case and in accordance with the results for Au_3, the linear structure is the lowest-energy isomer. For the tetramer, the most stable structure is the planar C_{2v} structure. For the pentamer, the extra electron stabilizes the C_{2v} structure, which becomes the ground state. Our findings for the VDEs of Pt_4 and Pt_5 are in good agreement with experiment [15,16], with a 0.2–0.3 eV overestimation in both LDA and BLYP. Pt_3 turns out to be a particularly interesting case because the two isomers have VDE values that differ by a large amount ($\sim$1.1 eV). Also the photoemission spectrum of Pt_3^- [15] is special among the Pt clusters spectra in that it has a low-intensity signal at the onset, at 1.9 eV, and a steep rise of the signal at 3.1 eV. Our results suggest that the cluster beam may indeed contain both isomers. This implies that the VDEs of small ground-state Pt clusters do not decrease monotonically as reported, for example, in Ref. [16].

3.3. Comparison Au–Pt microclusters

Gold and platinum microclusters in the range considered here ($n = 3, 4, 5$) prefer planar structures. In the case of Au, this is not surprising because previous studies on gold and also on the other noble-metal clusters came to the same conclusions. For example, the LSDA–LCGTO calculations of Cu clusters in Ref. [57] predict the D_{2h} and the planar C_{2v} isomers to be lowest in energy for Cu_4 and Cu_5, respectively. One-electron relativistic effective core potential calculations at the CASSCF level for silver clusters [48] report the same lowest-energy isomers. As discussed above, planar structures for the tetramer and the pentamer are also typical of alkali-metal aggregates and could be regarded as a sign that the contribution of the d-atomic states to the relevant bonding orbitals is negligible.

In contrast, the strong preference for planar structures found here for the platinum tetramer and pentamer does not agree with previous reports on small clusters of isolectronic elements, namely Ni and Pd. In fact, DFT calculations for nickel clusters [58] predict 3D structures for the ground-state structures of both tetramer and pentamer. These calculations include gradient-corrected xc functionals and use a linear combination of Gaussian orbitals as basis set. More specifically, Ni_3 is an equilateral triangle (triplet), as for Pt_3, but Ni_4 is a distorted tetrahedron with D_{2d} symmetry (quintet), and Ni_5 a trigonal bipyramid (quintet). For Ni_4 both the planar rhombus and the square were found to be metastable at energies 0.4 and 1.0 eV higher than the ground state. In the case of Pd, the trimer [59] and tetramer [42] have been investigated at the MRSDCI level of theory. The trimer was determined to be an isosceles triangle (singlet), and the tetramer a regular tetrahedron (triplet). However, for a comparison of Ni, Pd and Pt clusters to be valuable and conclusive, it should be carried out within one theoretical and computational framework. This is still lacking.

As expected, for both the Au and Pt clusters we find a contraction of the bond distance with respect to the nearest-neighbor distance of the solid. Our calculated value in bulk gold [60], [5] is 5.67 a.u. in BLYP and 5.42 a.u. in LDA (the experimental value is 5.44 a.u.); in bulk Pt it is 5.38 a.u. in BLYP and 5.18 a.u. in LDA (the experimental value = 5.24 a.u.). Thus the contraction (10–15%) is similar in the two schemes, and also for the two elements.

Clear differences between the two elements are observed in the electronic structure. The energy width of the one-electron states (Figs. 2 and 3) is larger for the platinum clusters than for gold and, most important, the character of the HOMO and LUMO states is different in the two metals.

[5] The results are in convergence with respect to k-point sampling of the Brillouin zone.

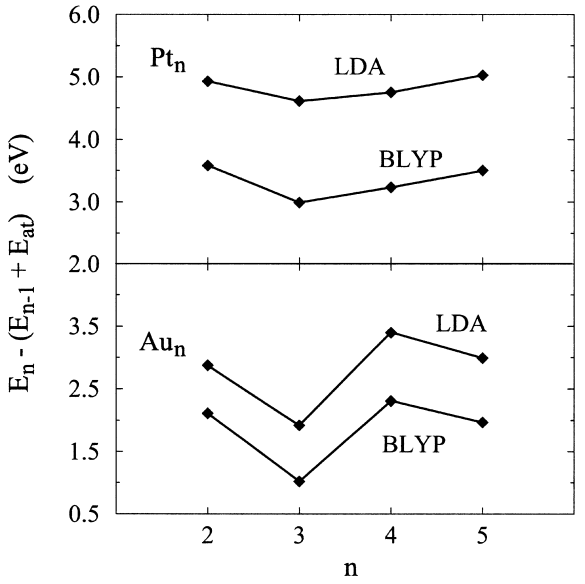

Fig. 5. Dissociation energies (in eV) of the clusters considered here, corresponding to fragmentation with loss of a monomer (E_{at}).

Whereas in gold clusters the states near the HOMO have predominantly s character, they have predominantly d character in those of platinum.

The computed fragmentation energies for monomer decay ($M_x \rightarrow M_{(x-1)} + M$) are shown in Fig. 5. The large difference between LDA and BLYP predictions is apparent. The pronounced even–odd alternation in gold clusters, typical of one-electron systems, is not mirrored by the platinum clusters, for which the variation is smooth.

4. Conclusions

This paper is intended as a contribution to our general understanding of metal clusters and to the performance of different methods. In particular, we have focussed on the structure, the electronic properties, the energy distribution of different isomers, and the effect of the addition of an electron as in the anions, and addressed issues such as the comparison of the LDA and BLYP approximations to DFT and the comparison of gold and platinum. Unfortunately, there is little input from experiment with which one can contrast theoretical predictions. The calculated values of the VDEs seem to agree well with experimental data on VDEs, especially for gold. However, one should take all this with care. In fact, VDEs are rather strongly dependent on the specific isomer, but because the theoretical findings are as strongly dependent on the xc functional used, one cannot use them as a confirmation of the computational scheme itself. This is well illustrated by the case of the gold tetramer, as discussed above.

Gaining more insight into the physics of heavy metal microclusters would highly profit from a systematic work of the type we have presented here, but extended to larger cluster sizes, additional DFT functionals, and other cluster properties. We believe that such a study is necessary if one wants to establish the appropriate theoretical approach to guarantee then that prediction and understanding of the chemistry of such aggregates are correct.

Acknowledgements

HG acknowledges a post-doctoral fellowship from STINT, and the kind hospitality of the IBM Zurich Research Laboratory. The calculations were performed on the IBM SP2 at PDC, Stockholm, Sweden.

References

[1] W. Ekardt (Ed.), Metal Clusters, Wiley, Chichester, 1999.
[2] P. Hohenberg, W. Kohn, Phys. Rev. 136 (1964) 864.
[3] W. Kohn, L.J. Sham, Phys. Rev. 140 (1965) A1133.
[4] P. Ballone, W. Andreoni, in: W. Ekardt (Ed.), Metal Clusters, Wiley, Chichester, 1999, pp. 71–144.
[5] Z. Xu, F.-S. Xiao, S.K. Purnell, O. Alexeev, S. Kawi, S.E. Deutsch, B.C. Gates, Nature 372 (1994) 346.
[6] A. Sanchez, S. Abbet, U. Heiz, W.-D. Schneider, H. Häkkinen, R.N. Barnett, U. Landman, J. Phys. Chem. A 103 (1999) 9573.
[7] F.C. Fritschij, H.B. Brom, L.J. de Jongh, G. Schmid, Phys. Rev. Lett. 82 (1999) 2167.
[8] T.G. Schaaff, R.L. Whetten, J. Phys. Chem. B 104 (2000) 2630.
[9] O. Dag, J. Phys. Chem. B 104 (2000) 6983.
[10] H. Häkkinen, R.N. Barnett, U. Landman, Phys. Rev. Lett. 82 (1999) 3264.

[11] W. Andreoni, A. Curioni, H. Grönbeck, Int. J. Quant. Chem., in press.
[12] H. Grönbeck, A. Rosén, W. Andreoni, Phys. Rev. A 58 (1998) 4630.
[13] C. Massobrio, A. Pasquarello, A. Dal Corso, J. Chem. Phys. 109 (1998) 6626.
[14] K.M. Ervin, J. Ho, W.C. Lineberger, J. Chem. Phys. 89 (1988) 4514.
[15] G.S. Icking-Konert, H. Handshuh, G. Ganteför, W. Eberhardt, Phys. Rev. Lett. 76 (1996) 1047.
[16] G. Ganteför, W. Eberhardt, Phys. Rev. Lett. 76 (1996) 4975.
[17] K.J. Taylor, C.L. Pettiette-Hall, O. Cheshnovsky, R.E. Smalley, J. Chem. Phys. 96 (1992) 3319.
[18] J. Ho, K.M. Ervin, W.C. Lineberger, J. Chem. Phys. 93 (1990) 6987.
[19] H. Handshuh, G. Ganteför, P.S. Bechthold, W. Eberhardt, J. Chem. Phys. 100 (1994) 7093.
[20] J.P. Perdew, A. Zunger, Phys. Rev. B 23 (1981) 5048.
[21] D.M. Ceperley, B.J. Adler, Phys. Rev. Lett. 45 (1980) 566.
[22] A.D. Becke, Phys. Rev. A 38 (1988) 3098.
[23] C.L. Lee, W. Yang, R.G. Parr, Phys. Rev. B 37 (1988) 785.
[24] R. Car, M. Parrinello, Phys. Rev. Lett. 55 (1985) 2471.
[25] N. Troullier, J.L. Martins, Phys. Rev. B 46 (1992) 1754.
[26] P. Carloni, W. Andreoni, M. Sprik, J. Phys. Chem. 104 (2000) 823.
[27] H. Grönbeck, W. Andreoni, Chem. Phys. Lett. 269 (1997) 385.
[28] H. Grönbeck, A. Curioni, W. Andreoni, J. Am. Chem. Soc. 122 (2000) 3839.
[29] S.G. Louie, S. Froyen, M.L. Cohen, Phys. Rev. B 26 (1982) 1738.
[30] D. Strömberg, U. Wahlgren, Chem. Phys. Lett. 169 (1990) 109.
[31] O.D. Häberlen, N. Rösch, Chem. Phys. Lett. 199 (1992) 491.
[32] K. Balasubramanian, J. Chem. Phys. 87 (1987) 6573.
[33] W. Liu, C. van Wuellen, J. Chem. Phys. 110 (1999) 3730.
[34] B.H. Hess, U. Kaldor, J. Phys. Chem. 112 (2000) 1809.
[35] E. van Lenthe, A. van der Avoird, P.E.S. Wormer, J. Chem. Phys. 108 (1998) 4783.
[36] E. van Lenthe, E.J. Baerends, J.G. Snijders, J. Chem. Phys. 101 (1994) 9783.
[37] J.P. Perdew, Phys. Rev. B 33 (1986) 8822.
[38] R.N. Barnett, U. Landman, Phys. Rev. B 48 (1993) 2081.
[39] P. Pulay, Chem. Phys. Lett. 73 (1980) 393.
[40] J. Hutter, H.P. Lüthi, M. Parrinello, Comput. Mat. Sci. 2 (1994) 224.
[41] H. Wang, E.A. Carter, J. Phys. Chem. 95 (1992) 1197.
[42] D. Dai, K. Balasubramanian, J. Chem. Phys. 103 (1995) 648.
[43] G. Ortiz, P. Ballone, Phys. Rev. B 44 (1991) 5881.
[44] K.P. Huber, G. Herzberg, Constants of Diatomic Molecules, Van Nostrand Reinhold, New York, 1979.
[45] J.L. Martins, J. Buttet, R. Car, J. Chem. Phys. 78 (1983) 5646.
[46] K. Jackson, Phys. Rev. B 47 (1993) 9715.
[47] W. Andreoni, J.L. Martins, Surf. Sci. 156 (1985) 635.
[48] V. Bonačić-Koutecky, L. Češpiva, P. Fantucci, J. Koutecký, J. Chem. Phys. 98 (1993) 7981.
[49] J.A. Howard, R. Sutcliffe, B. Mile, Surf. Sci. 156 (1985) 214.
[50] K. Balasubramanian, M.Z. Liao, J. Chem. Phys. 86 (1987) 5587.
[51] U. Müller, K. Sattler, J. Xhie, N. Venkateswara, G.J. Raina, J. Vac. Sci. Technol. B 9 (1991) 829.
[52] S.K. Gupta, B.M. Nappi, K.A. Gingerich, Inorg. Chem. 20 (1981) 966.
[53] S. Taylor, G.W. Lemire, Y. Hamerick, Z.W. Fu, M.D. Morse, J. Chem. Phys. 89 (1988) 5517.
[54] P.J. Hay, W.R. Wadt, J. Chem. Phys. 85 (1985) 270.
[55] S.H. Yang, D. Drabold, J.B. Adams, P. Ordejon, K. Glassford, J. Cond. Matter 9 (1997) L39.
[56] J. Harris, Phys. Rev. B 31 (1985) 1770.
[57] K.A. Jackson, Phys. Rev. B 47 (1993) 9715.
[58] M. Castro, J. Jamorski, D.R. Salahub, Chem. Phys. Lett. 271 (1997) 133.
[59] K. Balasubramanian, J. Chem. Phys. 91 (1991) 307.
[60] H. Grönbeck, A. Curioni, W. Andreoni, unpublished result.
[61] J. Ho, M.L. Polak, K.M. Ervin, W.C. Lineberger, J. Chem. Phys. 99 (1993) 8542.